Electron-phonon relaxation dynamics of niobium metal as a function of temperature

Margarita Mihailidi, Qirong Xing, K. M. Yoo, and R. R. Alfano
Institute for Ultrafast Spectroscopy and Lasers, Departments of Physics and Electrical Engineering, The City College and the Graduate Center of the City University of New York, New York, New York 10031
(Received 4 June 1993; revised manuscript received 3 August 1993)

The electron-phonon relaxation process in niobium has been measured with pump-probe technique and compared with theory for ambient (initial) temperatures ranging from 292 to 7 K. The time it takes for the electrons to thermalize with phonons was found to decrease from 370 fs at 292 K to 250 fs at 7 K, while the electron-phonon coupling parameter g decreases with decreasing temperature.

Femtosecond pump-and-probe experiments have enabled scientists to investigate the dynamics of the electron-phonon interactions by generating transient nonequilibrium temperatures in metals with femtosecond laser pulses. The electron relaxation time of Cu, Au, Nb, and other metals has been determined[1-4] by transient thermoreflectance and thermotransmittance spectroscopy. There are three dominant contributions to the thermotransmittance signal. These are as follows.

(i) Electron-phonon collisions result in phonon population increase, and this shifts and warps the energy bands through electron-phonon interaction. The change in transmissivity due to phonon population increase $\Delta\Theta_l$ is

$$\Delta T_l = \sum_Q \frac{\partial T}{\partial n_Q}\frac{\partial n_Q}{\partial \Theta_l}\Delta\Theta_l \ , \tag{1}$$

where T stands for transmissivity, n_Q is the phonon distribution, Q is the phonon quantum number and Θ_l is the lattice temperature.

(ii) Lattice expansion causes shifts and warping in the electron energy bands through changes in one-electron potential, which in turn causes the Fermi level to shift. The change in transmissivity due to lattice expansion $\Delta T_{\rm exp}$ is

$$\Delta T_{\rm exp} = \frac{\partial T}{\partial a}\Delta a \ , \tag{2}$$

where Δa represents the lattice expansion.

(iii) Fermi level smearing which occurs as the electron temperature rises, and the tails of the Fermi-level distribution spread out in energy and open states below the Fermi level for transition.[5] The change in transmissivity due to Fermi-level smearing ΔT_e is

$$\delta T_e = \sum_k \frac{\partial T}{\partial f_k}\frac{\partial f_k}{\partial \Theta_e}\Delta\Theta_e \ , \tag{3}$$

where f_k is the electron distribution, k is the electron quantum number and Θ_e is the electron temperature.

As shown in Fig. 1 and demonstrated by past researchers[1,4] the electron and phonon temperatures do not track each other on a fs time scale. Therefore, one needs to know what temperature the thermotransmittance signal is related to in order to analyze the experiment. For the Fermi-level smearing to be observed, an interband transition has to be excited by the pump photon, involving either an initial or a final electron state close to the Fermi level. The absence of the sharp characteristic shape of the response when Fermi-level smearing is detected[1] leads to the conclusion that the two other contributions, namely, the electron-phonon collisions and the lattice expansion, are dominant and are responsible for the thermotransmittance signal. The contribution due to phonon population increase, Eq. (1), is related to the lattice temperature. We also assume that the contribution due to lattice expansion is only related to lattice temperature. This assumption was made because the transmissivity signal does not have the characteristic shape of the electron temperature versus time as displayed in Fig. 1. The success of the following theoretical analysis supports this assumption. In our case, the probe measures the lattice temperature. This has been demonstrated by Eesley before in the thermoreflectance and thermotransmittance measurements performed in Cu.[1]

In this paper, the electron-phonon relaxation time for different sample (initial) temperatures, and the temporal behavior of the electron-phonon coupling parameter in

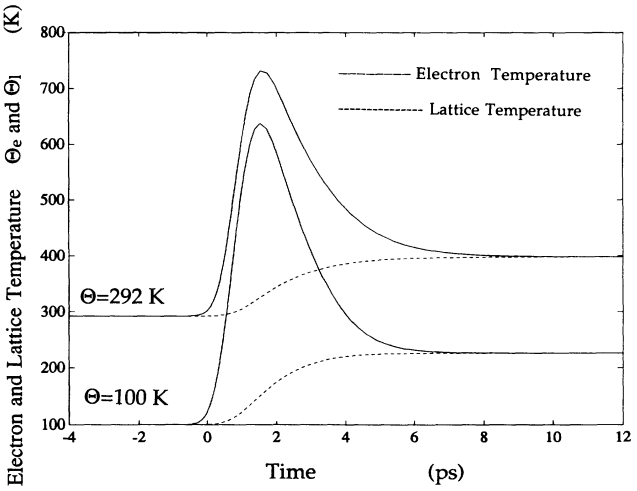

FIG. 1. The time evolution of electron (solid line) and lattice (dashed line) temperatures in Nb film computed numerically using Eqs. (3) and (4), for sample (initial) temperatures 292 and 100 K, for our experimental conditions.

Nb metal have been determined. The results are compared with Allen's theory for the thermal relaxation rate in a metal when the electrons are heated by ultrafast laser pulses above the temperature of the lattice.[6]

The heated electrons and phonons alter the dielectric constant, which in turn changes the transmissivity T as shown in the equations below:

$$\frac{\Delta T}{T}=\frac{1}{T}\left[\frac{\partial T}{\partial \varepsilon_1}\Delta\varepsilon_1+\frac{\partial T}{\partial \varepsilon_2}\Delta\varepsilon_2\right], \tag{4}$$

where $T=T(\tilde{n})$ and $\tilde{n}=\sqrt{\varepsilon_1+i\varepsilon_2}$. The change in the dielectric constant is known to be proportional to the change in both electric and lattice temperature[3,5] and therefore

$$\frac{\Delta T}{T}=a\Delta\Theta_l+b\Delta\Theta_e , \tag{5}$$

where $\tilde{n}$ is the index of refraction, a and b are constant coefficients, ε_1 and ε_2 are the real and the imaginary part of the dielectric constant, and Θ_e and Θ_l are the electron and lattice temperature, respectively. The thermotransmittance signal was caused by the lattice temperature increase, and it was measured to be linearly proportional to the laser fluence. Therefore, the normalized change in the transmittance $\Delta T/T$ is related to the change in the lattice temperature according to Eqs. (4) and (5).

The electrons are photoexcited with an ultrafast laser pulse source $S(r,t)$ where r is the space coordinate and t is time. These heated electrons transfer their energy to the lattice via electron-phonon interaction that is governed by the electron-phonon coupling parameter g. The evolution of the electron and lattice temperatures is described by coupled equations:[7]

$$C_e\frac{\partial\Theta_e}{\partial t}=k\nabla^2\Theta_e-g(\Theta_e-\Theta_l)+S(r,t) , \tag{6}$$

$$C_l\frac{\partial\Theta_l}{\partial t}=g(\Theta_e-\Theta_l) , \tag{7}$$

where k is the thermal conductivity, C_e and C_l are the electron and lattice heat capacity, respectively and $g=f(\Theta_e(t),\Theta_l(t))$.

Over a time scale of few picoseconds the electron-phonon interaction causes temperature relaxation $\delta\Theta_e/\delta t=-g/C_e(\Theta_l-\Theta_e)$. The pump pulse is ≤ 100 fs and the diffusion term may be neglected on the ps time scale.

The calculated time evaluation of temperatures Θ_e and Θ_l are displayed in Fig. 1 at sample temperatures 292 and 100 K. The time it takes for the electron to thermalize with the lattice τ (i.e., the lattice temperature rise time) increases with increasing C_l and decreases with increasing g. However, it is known that the rise time τ is also reduced with decreasing pump intensity $S(r,t)$, but is much more sensitive to the change in g than in $S(r,t)$.[4] The details, these calculations are based upon, are discussed below.

In the interpretation of this thermotransmittance experiment a one-dimensional heat flow model similar to other standard thin-film pump-probe experiments is used.[1] This is possible because the laser beam focal diameter ($d_{\text{pump}}=35$ μm) is large enough that the heat diffusion over the optical skin depth (~ 20 nm) dominates over radial diffusion out of the heated area during the time of interest (1.5 ps).

Diffusion in the direction of the pump beam is negligible during the time of our measurement, since the sample is thin enough compared to the optical skin depth at 625 nm. In the plane of the sample the distance traveled by the heat due to electron thermal diffusion may be estimated as $\Delta x=(D\Delta t)^{1/2}$, where $D=\kappa/C_e$ is the thermal diffusivity.[2] The diffusion parameters for Nb are $\kappa=55$ W m^{-1} K^{-1} and $C_e=2.2\times10^5$ Jm^{-3}K for $\Theta=300$ K, which gives $\Delta x<0.1$ μm for $\Delta t=1.2$ ps. The distance traveled due to diffusion becomes smaller as Θ increases. Therefore, for the duration of our measurements (1.2 ps) the increase in the excited area in the plane of the sample due to diffusion is negligible, since the laser focal diameter was $d=35$ μm, which is much less than $\Delta x=0.1$ μm.

The long temperature decay time due to diffusion is also demonstrated by the experiments performed for several metals (Ni, No, Ti, Zr, and Cu) by Clemens, Easley, and Paddock.[8] Using a transient thermoreflectance technique their measurements have shown that the temperature decay time due to diffusion is in the ns region.

Allen has derived an equation for the thermal relaxation rate in the high-T limit.[6] In this case, i.e., for temperatures greater than Debye temperature, Θ_D ($\Theta_D=275$ K for Nb), g may be considered temperature independent, and the thermal relaxation rate $-g/C_e$ has been related to the important electron-phonon mass enhancement parameter λ.[6] However, for temperatures close or smaller than Debye temperature there is no simple relation between g and λ.[6] The electron-phonon coupling parameter g in this case depends on the electron temperature Θ_e and phonon temperature Θ_l. To obtain a temperature dependent expression for $g(\Theta_e,\Theta_l)$ for temperatures $\leq\Theta_D$ the same approach and assumptions as Allen's are followed, starting from the expression for the rate of electron-phonon energy exchange $\delta E_e/\delta t$:[6]

$$\frac{\partial E_{ep}}{\partial t}=2\pi N(E_F)\int_0^\infty d\omega\,\alpha^2F(\omega)(\hbar\omega)^2 \times[N(\omega,\Theta_l)-N(\omega,\Theta_e)]. \tag{8}$$

In Eq. (8) $\alpha^2F(\omega)$ is the Éliashberg electron-phonon coupling function, $N(\omega,\Theta_l)$ and $N(\omega,\Theta_e)$ are the Bose-Einstein distributions for $\Theta=\Theta_l$ and $\Theta=\Theta_e$, respectively, and $N(E_F)$ is the electron density of states of both spins at the Fermi level. $N(E_F)$ in Eq. (5) is now substituted by $N(E_F)=3\gamma/\pi^2k_b^2$ obtained from the expression for the electron heat capacity C_e:

$$C_e=\frac{\pi^2k_b^2}{3}N(E_F)(1+\lambda)\Theta_e=\gamma(1+\lambda)\Theta_e , \tag{9}$$

where $(1+\lambda)$ is the electron-phonon enhancement factor

and γ is the electronic constant. For $\Theta_e > \Theta_D/3$ one may set λ to be equal to zero, while for $\Theta_e < \Theta_D/4$ it resumes its full value.[9]

Equation (8) is modified and equated to the expression for electron-phonon energy exchange

$$\frac{\partial E_e}{\partial t} = g(\Theta_e,\Theta_l)(\Theta_l - \Theta_e). \tag{10}$$

Thus, the time evolution of g occurs through time dependence of $\Theta_e(t)$ and $\Theta_l(t)$:

$$g(\Theta_e(t),\Theta_l(t)) = \frac{6\gamma\hbar^2}{\pi k_b^2(\Theta_l - \Theta_e)} \int_0^\infty d\omega\, \alpha^2F(\omega)\omega^2 \left\{ \left[\exp\left[\frac{\hbar\omega}{k_B\Theta_l} \right] - 1 \right]^{-1} - \left[\exp\left[\frac{\hbar\omega}{k_b\Theta_e} \right] - 1 \right]^{-1} \right\}. \tag{11}$$

Equations (6), (7), and (11) are numerically solved and the temperature dependence of the electron specific heat, lattice specific heat and the electron-phonon coupling is accounted dynamically. In the time scale of 0–1.5 ps the diffusion term $k\nabla^2\Theta_e$ may be neglected. As shown in the flowgraph presented in Fig. 2, the theoretical simulations are performed for a whole range of ambient temperatures from 292 to 7 K (g being temperature dependent) and compared with experimental results. The obtained transient thermotransmittance measurements represent the lattice contribution to the thermomodulation signal since the probe energy used is not near the Fermi level energy, measured with respect to the top of the d band.[1,4]

The experimental setup used for our transient thermotransmittance spectroscopy consists of a colliding pulse mode-locked (CPM) dye laser and an amplifier pumped with a copper vapor laser operating at 6.5 kHz. The duration of the pulses generated is 100 fs full width at half maximum and the wavelength is centered at 625 nm. For the lock-in detection the pump beam was chopped in order to detect the difference in the transmitted intensity of the probe beam caused the by pump. The probe pulse used was 1% of the pump intensity. The energy of the pump pulse was 110 nJ and was focused onto a spot 35 μm in diameter. In our experiment the probe spot radius is about five times smaller than the pump spot radius in order to minimize diffusion effects. A motorized translational stage with 1-μm accuracy was used to delay the probe pulse with respect to the pump pulse. The probe beam was polarized perpendicular to the polarization of the pump beam to avoid the large coherent artifact which occurs when the probe beam is polarized parallel to the pump beam. The niobium film used was 20 nm thick, deposited on a fused quartz, and is attached to a heat sink whose temperature may be varied. The experimentally determined absorptivity was found to be ~5% of the incident laser energy.

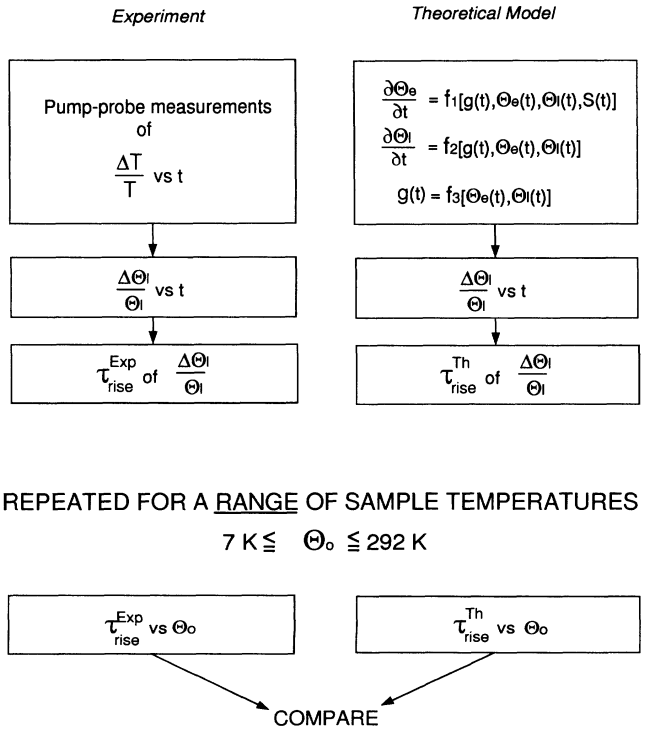

FIG. 2. The flowgraph presented describes the experimental and numerical procedure applied to obtain the electron-phonon thermalization time τ_{rise} for sample (initial) temperatures ranging from 292 to 7 K.

The change in transmitted probe intensity was measured for time delays from 0 to 1.5 ps of the probe pulse with respect to the pump. These measurements were performed for ambient temperatures from 292 to 7 K. The maximum change was 8% and was linearly dependent on the laser fluence. In these measurements, the fast purely electronic component was not observed because the probe wavelength was away from the electronic transition to the Fermi level. Therefore, the observed transmission change is attributed to the change in lattice temperature and is assumed to be linearly proportional.[1,4]

In Fig. 3 the measured relative transmission change is displayed for three different ambient temperatures, 292, 20, and 7 K for delays from −0.4 to 1.2 ps. The dashed line represents experimental data, and the dash-dotted line represents the best fit to the experimental data. The solid line represents the lattice temperature, computed using Eqs. (6), (7), and (11). The electron-phonon coupling parameter $g(\Theta_e,\Theta_l)$ from Eq. (11) is calculated for every time-step as values of Θ_e and Θ_l change, using an experimentally obtained electron-phonon coupling function $\alpha^2F(\omega)$.[10] The Debye theory approximation is used to calculate C_l at temperatures where there is good agreement with experimentally obtained C_l values for Nb. Otherwise, the experimentally obtained C_l values given in literature are directly used.[11] Electron heat capacity C_e is calculated using Eq. (9) with values for the electronic

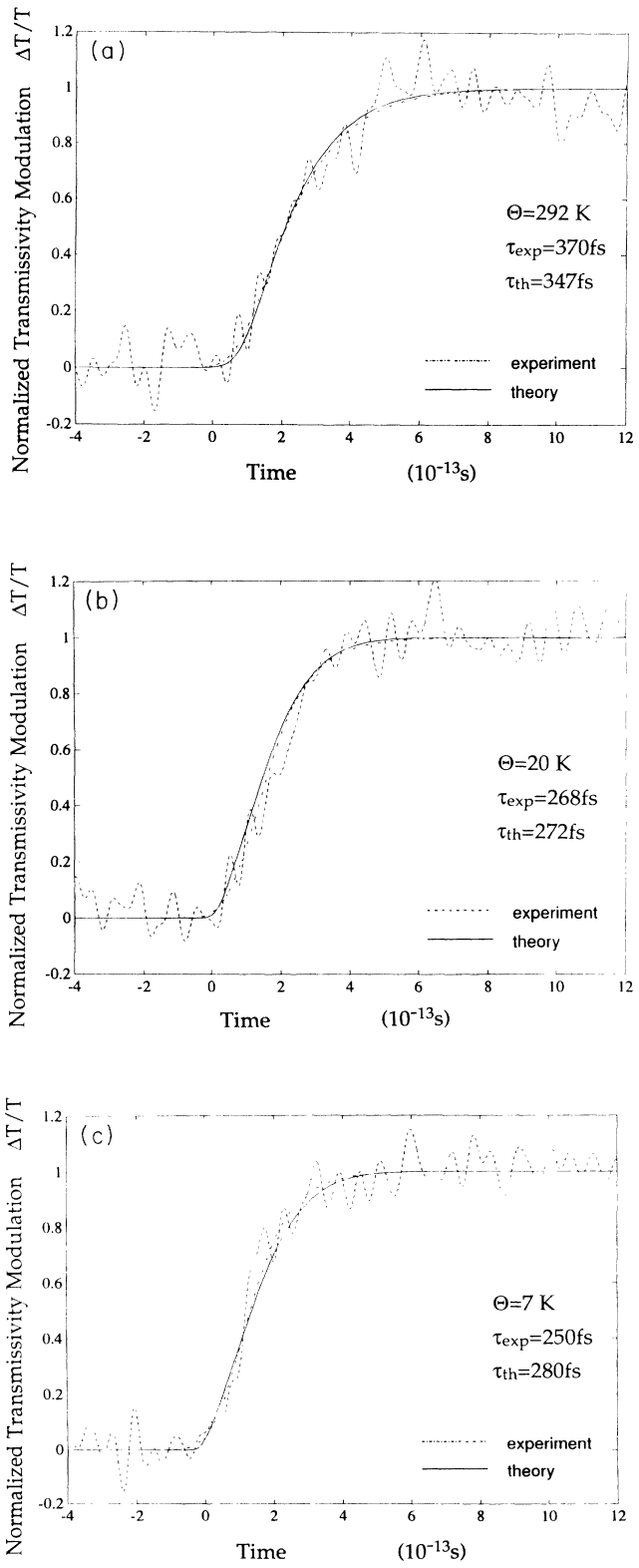

FIG. 3. The measured relative transmission change is displayed for three different sample temperatures 292, 20, and 7 K for delays from −0.4 to 1.2 ps. The dashed line represents experimental data, and the dash-dotted line represents the best fit to the experimental data. The solid line represents the lattice temperature, computed using Eqs. (3), (4), and the temperature dependent $g(\Theta_e,\Theta_l)$ according to Allen's theory, Eq. (8).

constant[12] $\gamma=719$ $\mathrm{Jm^{-3}K^{-2}}$ and the dimensionless electron-phonon mass enhancement parameter[13] $\lambda=0.82$, which vanishes at higher temperatures.[9] The displayed results for 292 and 20 K show fairly good agreement with theory, while the experimental result for 7 K shows a faster rise time than predicted by existing theory.[6]

Figure 4 shows the measured rise time (the time required to establish temperature equilibrium between the electrons and the phonons) as a function of sample temperature. The rise time (measured from 10 to 90 % of the total rise) decreases from 370 fs at 292 K to 250 fs at 7 K. The error bars reflect the standard deviation. Also plotted (solid circles) are values for the electron phonon relaxation time τ obtained from the numerical solution of Eqs. (6) and (7) when the temperature dependence of $g(\Theta_e,\Theta_l)$ [according to Eq. (11) derived from Allen's theory[6]] is included. Calculated values show rather good agreement with measured experimental values, undershooting the experimentally obtained τ by $<10\%$, from room temperature to well below Debye temperature ($\Theta_D=275$ K for Nb) at 20 K. However, for sample temperatures below 20 K the theoretical calculations give larger values of the transmissivity rise time than the experiment by about 15%, which means that the calculated coupling parameter $g(\Theta_e,\Theta_l)$ is too small at very low temperatures. When the convolution with the probe pulse is taken into account the actual experimentally obtained τ would be 5–10 % smaller than displayed in Fig. 4. The effect being greater for shorter τ, i.e., at smaller temperatures. This improves the agreement with theory at all but the lowest temperatures. However, the discrepancy between theory and experiment is greater at very low temperatures. The lower values and continuous decrease of the electron-phonon relaxation obtained from the experiment for $\Theta\leq\Theta_D/3$ are most likely due to a shake-off process taking place for $\Theta<\Theta_D/3$. Namely, at $\Theta<\Theta_D/3$ some part of the lattice energy is stored in a

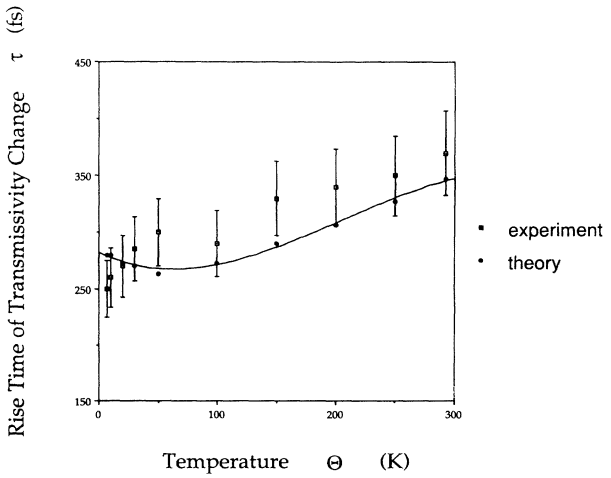

FIG. 4. Measured transmission rise time as a function of sample temperature. The rise time decreases from 370 fs at 292 K to 250 fs at 7 K. Also plotted are values for the lattice temperature rise time (i.e., the electron phonon relaxation time) obtained from the numerical solution of Eqs. (3) and (4) when the temperature dependence of g is included.

Fermi liquid, which is seen in the specific heat change from C_e to $(1+\lambda)C_e$. The laser pump pulse heats the electrons quickly from $\Theta_e=\Theta_a \ll \Theta_D$ to $\Theta_e > \Theta_D$. It causes a shake-off process leading to a release of the lattice energy represented by λ. So the absorbed energy is shared by the electrons and the shake-off phonon. This is an additional and probably faster mechanism to heat the lattice phonons at $\Theta < \Theta_D/3$. Moreover, this effect is more pronounced at lower temperatures, since λ increases with decreasing temperature, which explains the measured continuous decrease in electron-phonon relaxation time obtained from the experiment. The disagreement between theory and experiment at very low temperatures may also be attributed to the uncertainty in the experimentally obtained value of the electron-phonon mass enhancement parameter λ used in this calculations, whose effect is much more important at low temperatures.[9]

The experimental accuracy is $\mp 10\,\%$ as shown in Fig. 4, and this is adequate to determine a decrease from 370 to 250 fs (as the ambient temperature is decreased from 292 to 7 K) of the time it takes for the electrons to thermalize with phonons. This is especially true if we note that the experimentally obtained rise time shows a steady decrease with decreasing temperature in all but one measurement (Fig. 4).

The calculated [according to Eq. (11)] time evolution of the electron-phonon coupling parameter $g(\Theta_e,\Theta_l)$ for our experimental conditions is displayed in Fig. 5 for ambient temperatures 7, 20, 10, and 292 K. The time evolution is due to the change of Θ_e and Θ_l in time as the electrons are first heated by the pump pulse and then transfer the heat to the lattice according to Eq. (3) and (4). The negative time in Fig. 5 represents the time before the electrons are heated by the pump pulse, i.e., the value of g at ambient temperature. For temperatures below Debye temperature ($\Theta_D=275$ K for Nb) $g(\Theta_e,\Theta_l)$ initially increases with time as Θ_e and Θ_l increase. Then, as the electrons thermalize with phonons, $g(\Theta_e,\Theta_l)$ slightly decreases and acquires a constant value (on the ps time scale) after the electrons and phonons have thermalized. Note the corresponding time evolution of Θ_e (solid line) and Θ_l (dashed line) for ambient (initial) temperatures $\Theta=100$ and 292 K in the inset. The very low initial value of g at 7 K points out to the breakdown of the model for very low temperatures.

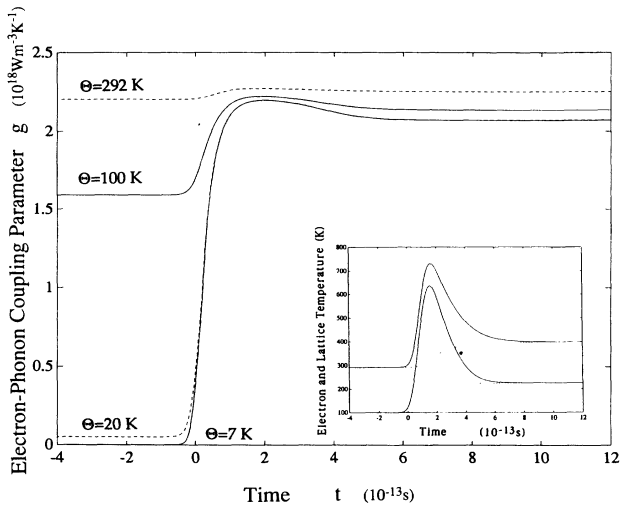

FIG. 5. The calculated time evolution of the electron-phonon coupling constant $g(\Theta_e,\Theta_l)$ for our experimental conditions is displayed for ambient temperatures 7, 20, 100, and 292 K. $g(\Theta_e,\Theta_l)$ increases with time as Θ_e and Θ_l increase and then slightly decreases as the electrons thermalize with phonons. Note the corresponding time evolution of Θ_e (solid line) and Θ_l (dashed line) for ambient (initial) temperatures $\Theta=100$ and 292 K in the inset. The close to zero value of g at 7 K also points out to the breakdown of the model for very low temperatures.

The results displayed in Fig. 5 confirm that the electron-phonon coupling parameter $g(\Theta_e,\Theta_l)$ is relatively constant for room temperature and above. g in Ref. 4 is estimated to be $1.7\mp 0.3\times 10^{18}$ W m^{-3} K^{-1}, while according to the present paper it is about 2.2×10^{18} W m^{-3} K^{-1} (with again a possible error of approximately $\mp 15\,\%$). One possible reason for this small difference may be that for room temperature measurements (as in Ref. 4) g is assumed constant which is only approximately so. According to Allens[6] theory in the high-temperature limit one can use the Taylor's series to derive the expression for g

$$g=\frac{3\hbar\gamma\lambda\langle\omega^2\rangle}{\pi k_B}\left[1+\frac{\hbar^2\langle\omega^4\rangle}{12\langle\omega^2\rangle k_p^2\Theta_e\Theta_l}+\cdots\right], \quad (12)$$

where

$$\lambda\langle\omega^n\rangle=2\int_0^\infty d\omega\left[\frac{\alpha^2F(\omega)}{\omega}\right]\omega^n . \quad (13)$$

Here, γ is the electronic constant, $\alpha^2F(\omega)$ is the Éliashberg electron-phonon coupling function and λ is the electron-phonon mass enhancement parameter which determines Θ_c and is the same as $\lambda\langle\omega^0\rangle$. For sufficiently high Θ_e and Θ_l only the first term is retained and g may be considered constant, but for room temperature measurements, keeping the second term of the Taylor series expansion may slightly change the shape of the lattice temperature rise. The difference in the two results for g is rather small and is not considered to be significant given the fact that the sample used in Ref. 4, although very similar, was not the same sample used in the present experiment.

In summary, the temporal behavior of the electron-phonon relaxation process (electron-phonon thermalization time) has been measured under nonequilibrium conditions and compared with theory for temperatures ranging from room temperature to below superconducting temperatures. It was found that the electron-phonon relaxation time decreases from 370 fs at 292 K to 250 fs at 7 K. The temperature dependence and time evolution of the electron-phonon coupling parameter $g(\Theta_e,\Theta_l)$ has been determined using Allen's theory. These values for $g(\Theta_e,\Theta_l)$ were used to obtain the numerically calculated rise time. The calculated electron-phonon relaxation time is in good agreement with the measured experimental values well below Debye temperatures, down to 20 K. This confirms the validity of the theoretical model for

$g(\Theta_e,\Theta_l)$ used for determining the time evolution of the electron-phonon coupling parameter. $g(\Theta_e,\Theta_l)$ was found to increase with Θ_e and Θ_l and the electrons thermalize with phonons faster at smaller ambient temperatures. No special features have been observed below superconducting temperature ($\Theta_c = 8.8$ K) on this time scale.

In work performed in the past[3,14,15] g used in Eqs. (3) and (4) has been referred to as the electron-phonon coupling constant and has been temperature independent since experiments were performed at room temperature. However, for temperatures $<\Theta_D$, when g becomes temperature dependent (and thus dependent on the intensity of the pump pulse) one should be aware that g is actually the coefficient of heat transfer between the electrons and the lattice.[7] The thermalization time τ is governed by the magnitude of g and by the electron and lattice heat capacities. It decreases with increasing g and decreasing specific heat. For temperatures $<\Theta_D$ both electron and lattice heat capacity decrease fast with temperature so the thermalization time diminishes as the temperature is lowered.

This work represents the first experimental evaluation of the existing theory developed by Allen. The experimentally obtained electron-phonon relaxation time for different ambient temperature was compared to the calculated ones, obtained based on existing theory, where the electron-photon parameter $g(\Theta_e,\Theta_1)$ is a function of electron and phonon temperatures. Reasonable agreement is obtained for temperatures down to 20 K. The agreement for the experiment with theory supports the validity of Allen's theory below Debye temperatures.

Although the difference between the experimentally obtained electron-phonon relaxation time and the theoretically calculated one is almost within the experimental error, it is clearly evident that for sample temperatures below 20 K the experimental results show a continuous decrease in the electron-phonon relaxation time, while according to the theory the relaxation time starts increasing slightly with temperatures $\Theta < 30$ K. There is a strong indication that the theoretical model has to be improved for temperatures from 30 K to below superconducting temperatures. The discrepancy seen at lower temperatures might be due to enhanced sensitivity to electron temperatures when the sample is held at lower temperatures. The temperature dependence of the electron-phonon mass enhancement parameter λ and the effect of the shake-off process that arise at lower temperatures also need to be addressed in more detail.

We would like to thank Professor J. Gersten, Professor J. L. Birman and Dr. A. Kuklov for helpful discussions on the theory and Dr. D. P. Osterman of HYPRES Inc. for the sample. This research has been supported by AFOSR.

[1]G. L. Eesley, Phys. Rev. B **33**, 2144 (1986).
[2]S. D. Brorson, J. G. Fujimoto, and E. P. Ippen, Phys. Rev. Lett. **59**, 1962 (1987).
[3]S. D. Brorson, A. Kazeroonian, J. S. Moodera, D. W. Face, T. K. Cheng, E. P. Ippen, M. S. Dresselhaus, and G. Dresselhaus, Phys. Rev. Lett. **64**, 2172 (1990).
[4]K. M. Yoo, X. M. Zhao, M. Siddique, and R. R. Alfano, D. P. Osterman, M. Radparvan, and J. Cunniff, Appl. Phys. Lett. **56**, 1908 (1990).
[5]R. Rosei and D. W. Lynch, Phys. Rev. B **5**, 3883 (1972).
[6]P. B. Allen, Phys. Rev. Lett. **59**, 1460 (1987).
[7]S. I. Asimov, B. L. Kopeliovich, and T. L. Perelman, Zh. Eksp. Teor. Fiz. **66**, 776 (1974) [Sov. Phys. JETP **39**, 375 (1974)].
[8]B. M. Clemens, G. L. Eesley, and C. A. Paddock, Phys. Rev. B **37**, 1085 (1988).
[9]Goran Grimvall, *Thermophysical Properties of Materials* (North-Holland, Amsterdam, 1986).
[10]G. B. Arnold, J. Zasadzinski, J. W. Osmun, and E. L. Wolf, J. Low Temp. Phys. **40**, 225 (1980).
[11]R. C. West and D. R. Lide, *CRC Handbook of Chemistry and Physics* (CRC Press, Boca Raton, 1990).
[12]Y. S. Touloukian and E. H. Buyvo, *Thermophysical Properties of Matter* (IFI/Plenum, New York, 1970), Vol. 3.
[13]B. N. Harmon and S. K. Sinha, Phys. Rev. B **36**, 2920 (1987).
[14]P. B. Corkum, F. Brunel, and N. L. Sherman, Phys. Rev. Lett. **61**, 2886 (1988).
[15]J. G. Fujimoto, J. M. Liu, and E. P. Ippen, Phys. Rev. Lett. **19**, 1837 (1984).